Journal of Catalysis **210,** 387–396 (2002)
doi:10.1006/jcat.2002.3688

Isotopic Transient Kinetic Analysis of Cs-Promoted Ru/MgO during Ammonia Synthesis

Brian C. McClaine and Robert J. Davis[1]

Department of Chemical Engineering, University of Virginia, Charlottesville, Virginia 22904-4741

Received February 25, 2002; revised May 17, 2002; accepted May 30, 2002

Steady-state isotopic transient kinetic analysis was used to examine a cesium-promoted Ru/MgO catalyst (1.75 wt% Ru) for ammonia synthesis. For comparison, an unpromoted Ru/SiO_2 (22 wt% Ru) catalyst was also studied. Steady-state and isotopic transient measurements were conducted at temperatures between 603 and 673 K with a stoichiometric ratio of N_2 and H_2 at a total pressure of 3 atm. The fractional surface coverage of nitrogen-containing intermediates (θ_{NH_x}) based on total H_2 chemisorption was found to range from 0.02 to 0.05 on both catalysts under the conditions used in the current study. However, the intrinsic turnover frequency of ammonia synthesis over Cs–Ru/MgO was two orders of magnitude greater than that of the unpromoted Ru/SiO_2. The combination of the Cs promoter and MgO support enhanced the intrinsic activity of Ru, presumably by lowering the barrier for dinitrogen dissociation.

Key Words: **ruthenium; ammonia, synthesis of; cesium, promotion by; SSITKA; isotopic transient analysis.**

INTRODUCTION

Although typical commercial catalysts for ammonia synthesis consist primarily of multipromoted iron ($Fe–Al_2O_3–CaO–K_2O$), interest in ruthenium has been renewed due to its higher activity. Since the production of ammonia from its elements is exothermic, an active ruthenium-based catalyst would allow operation at thermodynamically favored low temperatures and thus milder operating pressures. The generation of high pressure is an important component in the energy demand for conventional ammonia synthesis. In fact, the entire process of synthesizing ammonia requires approximately 1% of the world's power production (1). A promoted ruthenium catalyst supported on carbon was developed for use in the Ocelot Ammonia Plant in British Columbia. In addition to lower capital costs, the energy consumption of the plant was reduced by 1 million BTU/ton of ammonia produced compared to a typical iron-based system (2). However, the high cost and relatively short lifetime of a Ru/carbon catalyst compared to a conventional iron catalyst might outweigh the increase in activity (3).

[1] To whom correspondence should be addressed. E-mail: rjd4f@virginia.edu.

In addition to carbon, metal oxides have shown promise as supports for ruthenium-based catalysts due to their stability under ammonia synthesis conditions. In particular, Aika *et al.* have shown Ru/MgO to be an excellent catalyst for ammonia synthesis when promoted with Cs (4, 5). However, the role(s) of Cs as a promoter and MgO as a support for ruthenium-catalyzed ammonia synthesis has not fully been elucidated. Using N_2 temperature-programmed adsorption and desorption experiments, Hinrichsen *et al.* have shown that Cs enhances the rate constant of both dissociative adsorption and associative desorption (6). However, direct measurement of the effect of promoters on Ru ammonia synthesis catalysts under reaction conditions has been lacking.

The purpose of the current work was to determine surface coverage and lifetime of nitrogen-containing intermediates on a highly active Cs-promoted Ru/MgO catalyst under reaction conditions using steady-state isotopic-transient kinetic analysis (SSITKA). SSITKA is a powerful *in situ* technique for the kinetic study of heterogeneous catalytic reactions. The current method of SSITKA was first introduced to heterogeneous catalysis by Happel (7) and has been employed previously in the study of Fischer–Tropsch synthesis (8), CO hydrogenation (9–13), oxidative coupling of methane (14), ammonia oxidation (14), NO decomposition (14), and methanol synthesis (15, 16). The isotopic transient technique has also been used to study several catalysts for ammonia synthesis, including a commercial iron-based catalyst and a potassium-promoted, silica-supported ruthenium catalyst (17, 18).

The basic principle of SSITKA is the detection of isotopically labeled species versus time in the reactor effluent following a switch (step change) in the isotopic content of one of the reactant species without disturbing the overall steady-state reaction conditions. A mass spectrometer is used to record the resulting transient responses (formation or decay) of the labeled compounds (reactants and products) as they exit the reactor. Since the switch only involves changing the isotopic label of one of the reactants, isothermal and isobaric reaction conditions are maintained, and the reactant and product partial pressures and flow rates remain unchanged. Thus, in the absence of isotopic

0021-9517/02 $35.00

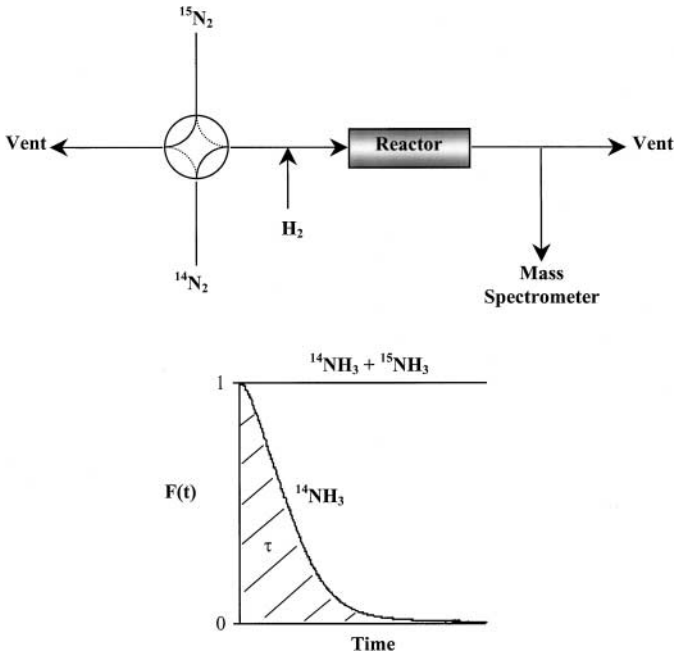

FIG. 1. Experimental setup for steady-state isotopic-transient kinetic analysis (SSITKA) and an example of a typical transient.

mass effects, steady-state reaction conditions are maintained throughout the switch. The information obtained from SSITKA may include surface coverage of different adsorbed reaction intermediates, lifetimes of surface intermediates, heterogeneity of active sites, and identification of possible reaction mechanisms. Generally, the clearest information is obtained from reactions that have a high surface coverage of slowly transforming reactive intermediates. A diagram of the reaction system and a typical normalized transient ($F(t)$) can be found in Fig. 1. It should be noted that $F_{^{14}NH_3}(t) = 1 - F_{^{15}NH_3}(t)$, as the sum of the two must equal unity in order to maintain the overall steady state. For additional information regarding the SSITKA technique, the reader is referred to the recent review by Shannon and Goodwin (19).

EXPERIMENTAL METHODS

Catalyst Preparation

A Cs–Ru/MgO sample was prepared by adding ruthenium (~2 wt%) onto magnesia (Ube Industries, 42 $m^2\ g^{-1}$) by impregnation with $Ru_3(CO)_{12}$ (Aldrich, 99%) dissolved in THF. The ruthenium was then reduced before addition of Cs. The sample was first dehydrated by heating under vacuum at 0.5 K min^{-1} to 723 K and maintained at that temperature for 1 h. The sample was then cooled to room temperature under vacuum and exposed to flowing H_2 (purified by diffusion through Pd, Matheson 8371V). The sample was subsequently heated in flowing H_2 (20 ml min^{-1} g^{-1}) at 1 K min^{-1} from room temperature to 723 K, held at temperature for 2 h, and finally cooled under vacuum (final pressure less than 10^{-5} Torr). Cesium was added as a promoter in a 1 : 1 atomic ratio with ruthenium by impregnation with aqueous cesium acetate. The acetate was decomposed by heating the catalyst in flowing N_2 (50 ml min^{-1} g^{-1}) at 1 K min^{-1} to 773 K.

An unpromoted Ru/SiO_2 sample (~20 wt% Ru) was prepared from Cab-O-Sil fumed silica as a reference material. The sample underwent the same ruthenium impregnation and reduction procedure described above for the MgO-supported catalyst. However, several impregnation and reduction steps were required to obtain the desired ruthenium loading.

Gas Adsorption

Dihydrogen chemisorption experiments were performed on a Coulter Omnisorp 100CX instrument. Before chemisorption, the sample was heated in vacuum at 2 K min^{-1} to 673 K, reduced in flowing dihydrogen (99.999% pure and further purified through an OMI-2 purifier) for 30 min at 668 K, and finally outgassed in high vacuum at 673 K for 45 min (final pressure less than 10^{-6} Torr). The sample was cooled in vacuum to room temperature for chemisorption. After chemisorption (total), the sample was evacuated at room temperature to remove weakly held hydrogen and a subsequent backsorption (reversible) isotherm was obtained. The amounts of total and reversibly adsorbed hydrogen were calculated by extrapolating the linear part of the adsorption isotherms to zero pressure. The amount of irreversibly adsorbed hydrogen was calculated from the difference between the total and the reversible isotherms. Hydrogen-based turnover frequencies (TOF_H) were based on irreversibly adsorbed hydrogen to be consistent with earlier work. However, ruthenium particle size and the fractional surface coverage of nitrogen-containing intermediates (θ_{NH_x}) were determined by total adsorbed hydrogen assuming a $H : Ru_{surface}$ ratio of 1 : 1.

X-ray Absorption Spectroscopy

The X-ray absorption spectra associated with the Ru K-edge (22,118 eV) for the Ru/SiO_2 sample was obtained at beam line X23A2 of the National Synchrotron Light Source (electron energy of 2.6 GeV and ring currents of 200–400 mA) at Brookhaven National Laboratory. The sample was first diluted in boron nitride (Alfa Aesar) and then pressed into a self-supporting pellet. The pellet was mounted in a cell capable of heating and cooling a sample in controlled atmospheres. The catalyst was heated at 5 K min^{-1} to 723 K while flowing dihydrogen at 50 ml min^{-1}. The sample was held at 723 K for 2 h and cooled in flowing dihydrogen to liquid dinitrogen temperature for collection of spectra. Additional details of the analysis procedure and results for the Cs-promoted Ru/MgO catalyst were reported previously (20).

Isotopic Transient during Ammonia Synthesis

Each catalyst was pressed under 1.5 metric tons, then crushed and sieved to between 250 and 425 μm. A 270-mg sample of Cs–Ru/MgO was loaded into a quartz microreactor (4-mm inside diameter) using quartz wool to hold the sample in place. The sample was heated at 2 K min^{-1} to 723 K in 40 ml min^{-1} of flowing N_2/H_2 (stoichiometric ratio) and held at 723 K for 2 h. The sample was then cooled to the desired temperature to measure reaction kinetics. Steady-state transient responses were collected at constant total flow rate (40 ml min^{-1}) as well as constant ammonia pressure ($P_{NH_3} = 0.0113$ atm) at various temperatures. The total flow rate was also varied between 20 and 40 ml min^{-1} at 638 K to examine the effect of ammonia readsorption on the catalyst particles. Mass flow controllers were used to control the flow rates of the gases, and all switches were performed under stoichiometric conditions and a total pressure of 3 atm.

A similar loading (275 mg) and reduction procedure was used for the unpromoted Ru/SiO_2 sample. However, due to its low activity, only transient responses at 673 K (20 and 40 ml min^{-1}) with a total pressure of 3 atm were collected.

Normal dinitrogen ($^{14}N_2$) containing a trace amount of argon (1.06%) was further purified by passage through a Supelco OMI-2 purifier. Argon was included in order to determine the gas-phase holdup of the reactor system. The concentration of Ar was not sufficient to disturb the steady-state during the switches. To ensure the same level of purity, the labeled dinitrogen (98+%, $^{15}N_2$, Isotec) was also purified by passage through a Supelco OMI-2 purifier. Dihydrogen (99.999%) was purified by diffusion through a Pd membrane (Matheson 837IV).

The isotopic transient responses were acquired by switching between different feed streams of isotopically labeled dinitrogen ($^{14}N_2/Ar \rightarrow {}^{15}N_2$). To reduce the amount of gas being switched, dihydrogen was introduced into the system after the switching valve. An electronically operated pneumatic valve was used for switching between normal and labeled streams. A perturbation-free switch was accomplished by use of backpressure regulators which maintained the reactor and vent lines at the same pressure. The concentrations of $^{14}NH_2$, $^{14}NH_3$, $^{15}NH_3$, $^{14}N_2$, $^{14}N^{15}N$, $^{15}N_2$, and Ar ($m/e = 16$, 17, 18, 28, 29, 30, and 40, respectively) were continuously monitored by a Balzers–Pfeiffer Prism 200-amu mass spectrometer. The mass spectrometer housing and transfer lines were maintained at 443 K to minimize ammonia adsorption. The signal for $^{14}NH_2$ ($m/e = 16$) was monitored due to the level of fragmentation that resulted from an electron excitation energy of 40 eV. The reverse switch was performed ($^{15}N_2 \rightarrow {}^{14}N_2/Ar$) in a similar manner. The mass spectrometer was calibrated for ammonia pressure by monitoring the effluent of the reactor that achieved thermodynamic equilibrium.

No evidence of ammonia formation was found in an empty reactor under typical reaction conditions. However, holdup of ammonia was observed when the empty reactor was subjected to a step change in ammonia concentration, resulting in a characteristic τ_{NH_3} associated with the system.

RESULTS

Table 1 contains results found from elemental analysis and dihydrogen chemisorption. The total hydrogen chemisorption results were used to calculate the average particle diameter of the ruthenium clusters, $d_{p,C}$. Also listed in Table 1 are structural parameters determined from Ru *K* edge EXAFS analysis. The Fourier transform and a comparison between the experimental and fitted EXAFS function for the Ru/SiO_2 catalyst are presented in Fig. 2. The coordination numbers found from EXAFS analysis were also used to calculate the average particle diameters $d_{p,E}$, with a good agreement achieved with the results based on total hydrogen chemisorption (21, 22). The high dispersion (0.54) of the Ru/SiO_2 sample was rather surprising given the loading of ruthenium (21.9 wt%). However, this is consistent with results found by Gao and Schmidt for a 5 wt% Ru/SiO_2 sample. Using transmission electron microscopy, they found particles in the range of 10–30 Å, and only after heating above 873 K did sintering occur (23).

Arrhenius-type plots at constant flow rate (40 ml min^{-1}, Runs 1–3 in Table 2) and constant ammonia pressure (0.0113 atm, Runs 4–6) for the Cs–Ru/MgO catalyst based on steady-state measurements (TOF_H) can be found in Fig. 3. The turnover frequency was based on the ammonia production rate divided by the number of sites counted by irreversible H_2 chemisorption. The apparent activation energy was 120 kJ mol^{-1}, which is consistent with values found previously at higher pressure (24, 25). By varying the total flow rate of reactants, the ammonia reaction order was found to be nearly zero (−0.06). Similar results were found earlier in our lab and elsewhere for an identical catalyst (24, 26).

TABLE 1

Characterization Results of Supported Ruthenium Catalysts

Catalyst	wt% Ru	N_{Ru-Ru}[a]	R_{Ru-Ru}[a]	H/Ru_{tot}	H/Ru_{irr}	$d_{p,E}$[b] (nm)	$d_{p,C}$[c] (nm)
Cs–Ru/MgO	1.75	8.4	2.69[d]	0.95	0.63	0.8–1.0	1.0
Ru/SiO_2	21.9	10.4	2.69	0.54	0.37	2.0–2.7	1.9

[a] Coordination number (N) and interatomic distance (R) from EXAFS analysis.

[b] Particle size based on results from EXAFS (21, 22).

[c] Particle size based on results from total H_2 chemisorption.

[d] Published previously in Ref. (20).

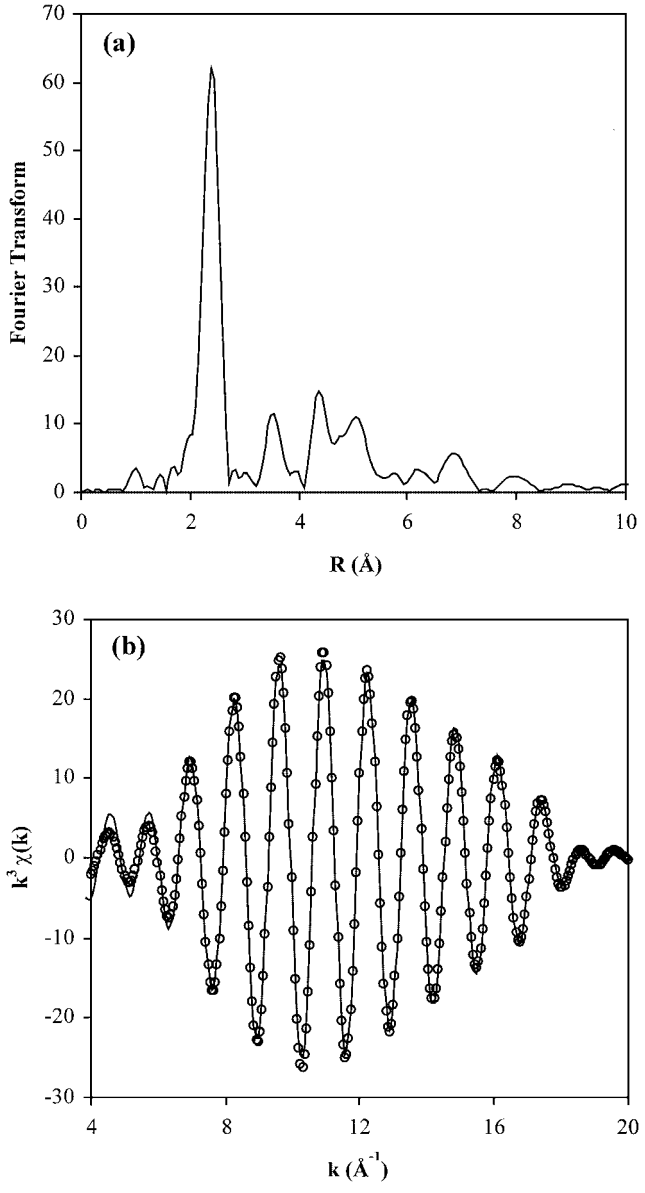

FIG. 2. (a) Radial structure function (Fourier transform) not corrected for phase shift and (b) observed and fitted Ru *K*-edge back transforms for Ru/SiO_2. The sample was reduced in flowing H_2 at 723 for 2 h and cooled to liquid dinitrogen temperature prior to data acquisition.

A typical set of normalized isotopic transients for $^{15}NH_3$ and Ar obtained for the Cs–Ru/MgO catalyst at 673 K and 40 ml min^{-1} (Run 3, Table 2) following a switch from $^{14}N_2$/Ar to $^{15}N_2$ can be found in Fig. 4. Also shown in Fig. 4 is an example of a blank curve following a switch from $NH_3/N_2/H_2$ to N_2/H_2 under similar conditions. For clarity, not all points for each curve are shown in Fig. 4. As can been seen from the transients, gas phase holdup is negligible but ammonia readsorption in the system needs to be accounted for in the final analysis. The average residence time of surface intermediates leading to ammonia (τ_{NH_3}) was calculated by integrating the area between the normalized transients,

TABLE 2

NH_3 SSITKA Results for Cs-Promoted Ru/MgO Catalyst

Run	T (K)	Flow rate (ml min^{-1})	P_{NH_3} (atm)	TOF_H[a] (10^{-4} s^{-1})	τ_{NH_3}(s)	θ_{NH_x}[b]	TOF_{intr}[c] (10^{-4} s^{-1})
1	603	40	0.003	9	27	0.017	370
2	638	40	0.013	40	11	0.030	880
3	673	40	0.035	109	7.1	0.051	1410
4	618	16	0.012	14	22	0.021	460
5	638	40	0.011	34	10	0.022	1010
6	668	100	0.011	89	5.5	0.032	1840
7	638	20	0.021	33	12	0.026	830
8	638	30	0.015	34	12	0.027	840
9	638	40	0.011	34	10	0.022	1000

[a] Based on irreversible H_2 chemisorption.
[b] Based on total H_2 chemisorption.
[c] Calculated from $1/\tau_{NH_3}$.

$$\tau_{NH_3} = \int_0^\infty \left[F_{^{14}NH_3}(t) - F_{^{blank}NH_3}(t)\right] dt, \qquad [1a]$$

$$\tau_{NH_3} = \int_0^\infty \left[1 - F_{^{15}NH_3}(t) - F_{^{blank}NH_3}(t)\right] dt, \qquad [1b]$$

where $F_{^{14}NH_3}$, $F_{^{15}NH_3}$, and $F_{^{blank}NH_3}$ are the normalized transient responses for $^{14}NH_3$, $^{15}NH_3$, and the corresponding blank, respectively. The number of surface intermediates,

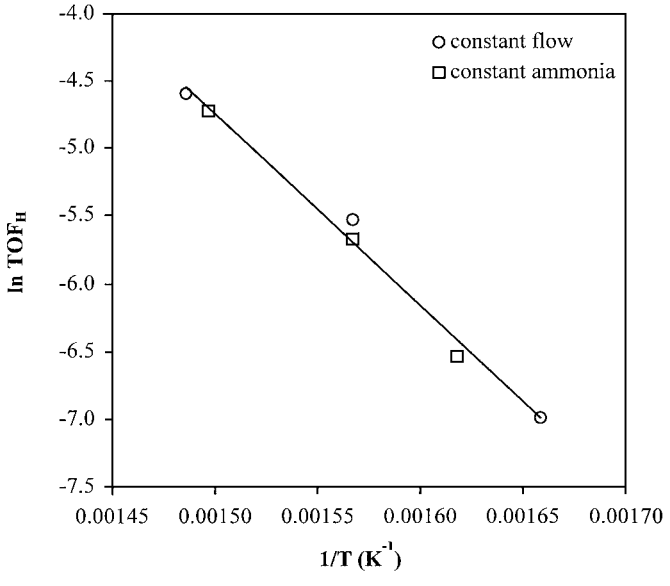

FIG. 3. Arrhenius-type plot for Cs-promoted Ru/MgO catalyst at constant flow rate (40 ml min^{-1}) and constant ammonia pressure ($P_{NH_3} = 0.011$ atm). Total pressure was 3 atm. The apparent activation energies were found to be 116 and 124 kJ mol^{-1} for constant flow rate and constant ammonia pressure, respectively.

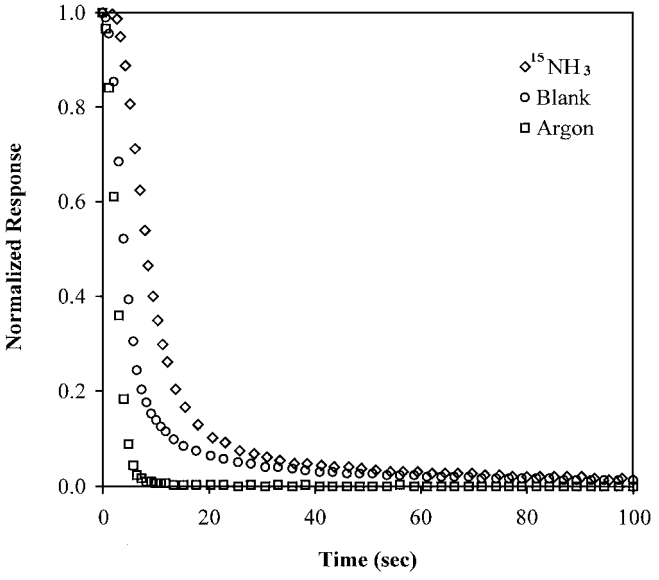

FIG. 4. Typical isotopic transients of $^{15}NH_3$ and Ar as a function of time at 673 K and 40 ml min^{-1} for Cs–Ru/MgO catalyst at 3 atm. Also shown is an example of a blank under similar reaction conditions. For clarity, not all points are shown.

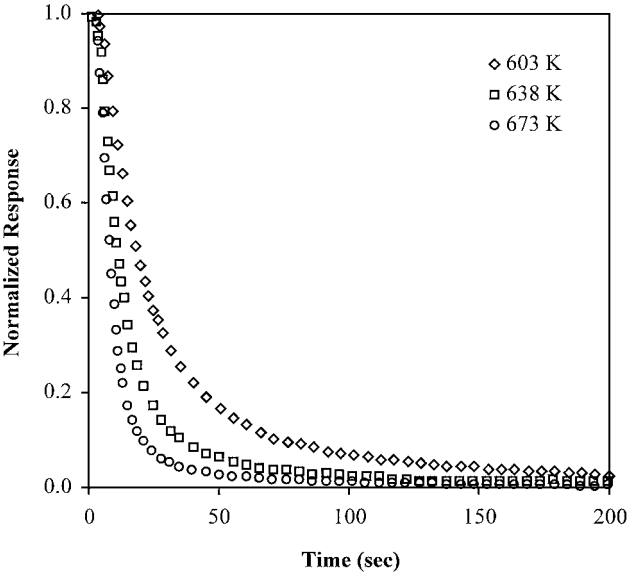

FIG. 5. Normalized transients of $^{15}NH_3$ at various temperatures at constant flow rate (40 ml min^{-1}) for Cs–Ru/MgO. For clarity, not all points are shown.

N_{NH_x}, leading to ammonia was then determined from

$$N_{NH_x} = \tau_{NH_3} R_{NH_3}, \quad [2]$$

where R_{NH_3} is the steady-state rate of ammonia formation per gram of catalyst. The fractional coverage of nitrogen-containing species on the ruthenium particles can be calculated from the results of dihydrogen chemisorption.

The effect of temperature on the isotopic transients at constant flow rate (ammonia partial pressure varied from 0.003 to 0.035 atm; Runs 1–3, Table 2) is demonstrated in Fig. 5. As expected, the area under the normalized transients decreased with increasing temperature of the reactor. Since the intrinsic turnover frequency is defined as

$$\mathrm{TOF}_{\mathrm{intr}} = 1/\tau_{NH_3}, \quad [3]$$

the intrinsic activation energy can be obtained by plotting $\mathrm{TOF}_{\mathrm{intr}}$ as a function of inverse temperature. The intrinsic activation energy was found to be 80 kJ mol^{-1} if the constant-flow-rate point at 673 K was neglected due to its proximity to equilibrium. Constant-flow measurements do not account for the order of magnitude increase in ammonia pressure. Results obtained at constant ammonia pressure (0.0113 atm; Runs 4–6, Table 2), also shown in Fig. 6 (squares), were similar to those at constant flow rate, which is consistent with a nearly zero-order dependence on ammonia. The intrinsic activation energy in this case was found to be 94 kJ mol^{-1}. These values are slightly lower than the apparent activation energy determined from data in Fig. 3.

Readsorption on both active and inactive sites can cause an overestimation of the average surface residence times and, therefore, the concentration of active sites obtained by SSITKA. Readsorption has been found to be a function of the partial pressure and flow rate in methanol synthesis (10, 15, 16). The effect of interparticle readsorption of ammonia was therefore examined by varying the total flow rate between 20 and 40 ml min^{-1} at 638 K (Runs 7–9, Table 2).

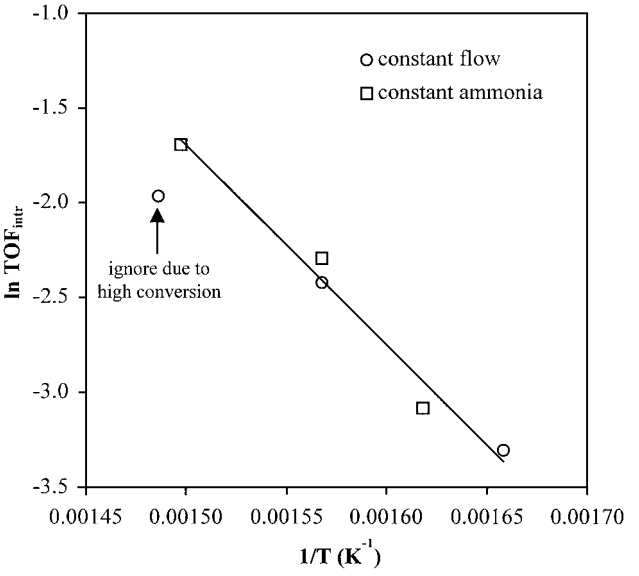

FIG. 6. Arrehenius-type plot of the intrinsic turnover frequency ($\mathrm{TOF}_{\mathrm{intr}}$) as determined from SSITKA at constant flow rate and constant ammonia pressure for Cs–Ru/MgO.

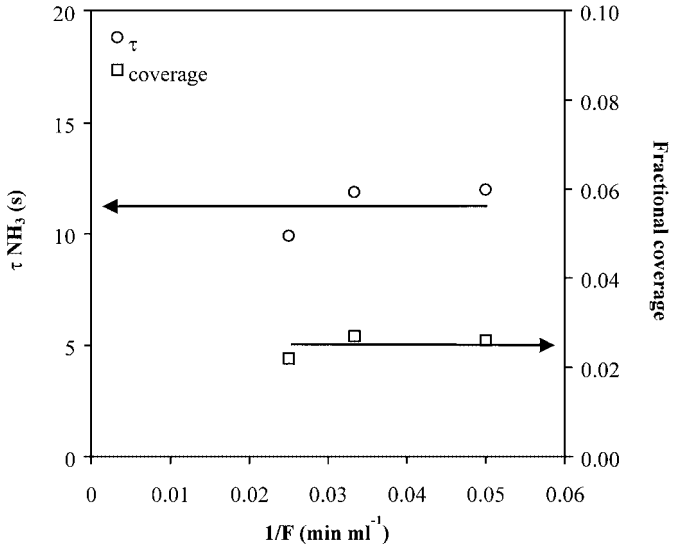

FIG. 7. Effect of flow rate (ammonia readsorption) on determination of SSITKA parameters.

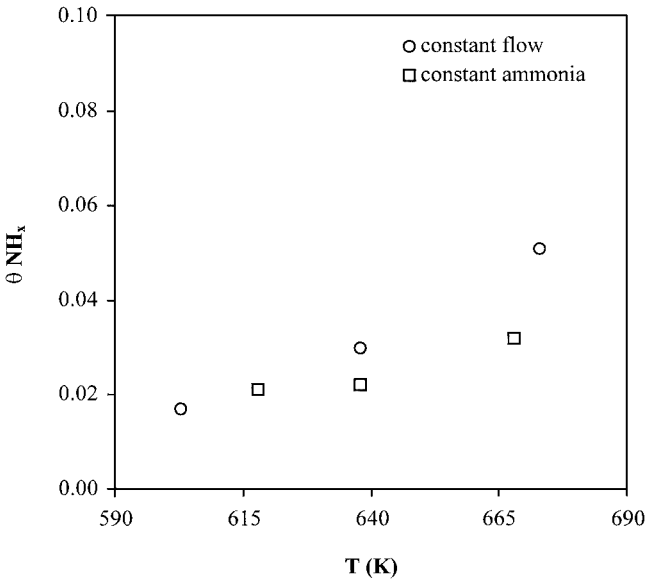

FIG. 8. Fractional surface coverage of nitrogen-containing intermediates (θ_{NH_x}) as a function of temperature for Cs–Ru/MgO catalyst at constant flow rate (40 ml min^{-1}) and constant ammonia pressure ($P_{NH_3} = 0.011$ atm).

The effect of flow rate on τ_{NH_3} (circles) and fractional coverage (squares) can be seen in Fig. 7. It should be noted that by doubling the total flow rate, the value of τ_{NH_3} changed by less than 20%. However, higher partial pressures of ammonia should result in a more accurate measure of τ_{NH_3} because of the increase in competition for readsorption (10). As can be seen from Fig. 7, the effect of total flow rate had a very small effect on τ_{NH_3} at 638 K under the conditions examined. All measured values of τ_{NH_3} are therefore assumed to be independent of ammonia readsorption and thus represent a good approximation of the intrinsic activity ($1/\tau_{NH_3}$) of the active sites.

The effect of temperature on the fractional coverage of nitrogen-containing species (θ_{NH_x}) at both constant flow rate (circles) and constant ammonia pressure (squares) can be seen in Fig. 8. The increase in fractional coverage with temperature at constant flow rate is not surprising since the partial pressure of ammonia was higher at higher temperatures due to an increase in rate. In fact, the ammonia pressure varied by an order of magnitude over the temperature range studied. To remove the influence of ammonia pressure on the surface coverage of nitrogen-containing species, the total flow rate was adjusted to obtain the same outlet pressure of NH_3 ($P_{NH_3} = 0.011$ atm) at each temperature. Figure 8 shows that the coverage varied from 0.021 to 0.032, independent of temperature. More important, the magnitude of θ_{NH_x} is quite small, suggesting that a very small fraction of the ruthenium surface is active for dinitrogen dissociation and ammonia synthesis. The results from the SSITKA experiments for the Cs–Ru/MgO catalyst under the variety of conditions examined are summarized in Table 2.

Results from analysis of a 22 wt% Ru/SiO_2 catalyst are found in Table 3. A comparison between normalized transients for Cs–Ru/MgO and Ru/SiO_2 at 673 K and 40 ml min^{-1} is found in Fig. 9. Due to the low activity of the catalyst, temperatures below 673 K were not examined. For Ru/SiO_2, there was a 20% change in τ_{NH_3} upon doubling the flow rate. This result was anticipated given the large number of surface ruthenium atoms on which readsorption of ammonia can occur. The intrinsic turnover frequency (TOF_{intr}) over Ru/SiO_2 was 0.0017 s^{-1} when extrapolated to infinite flow rate. This value is two orders of magnitude lower than the intrinsic turnover frequency found for the cesium-promoted Ru/MgO catalyst at the same temperature (Run 3, $TOF_{intr} = 0.14$ s^{-1}). On the other hand, both catalysts had almost the same surface coverage of nitrogen-containing intermediates (less than 6%) even though the ammonia pressure was an order of magnitude higher over the Cs–Ru/MgO.

TABLE 3

NH_3 SSITKA Results for Ru/SiO_2 Catalyst

T (K)	Flow rate (ml min^{-1})	P_{NH_3} (atm)	TOF_H[a] (10^{-4} s^{-1})	τ_{NH_3}(s)	θ_{NH_x}[b]	TOF_{intr}[c] (10^{-4} s^{-1})
673	20	0.0039	0.81	800	0.044	13
673	40	0.0016	0.65	670	0.030	15

[a] Based on irreversible H_2 chemisorption.
[b] Based on total H_2 chemisorption.
[c] Calculated from $1/\tau_{NH_3}$.

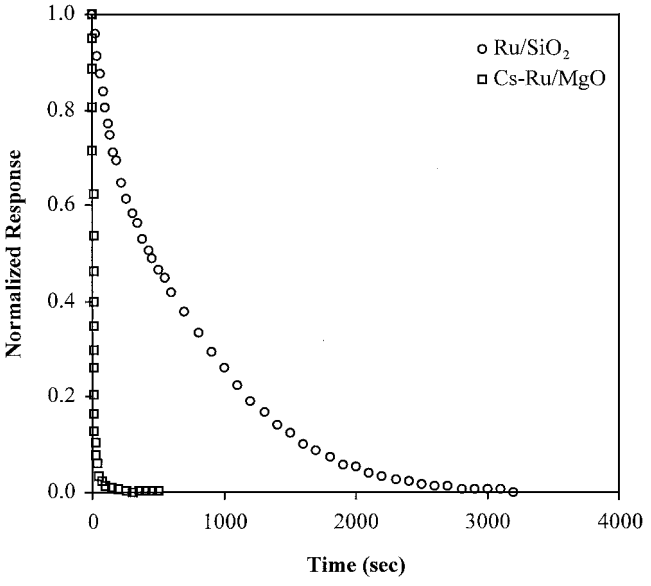

FIG. 9. Normalized transients of $^{15}NH_3$ as a function of time at 673 K and 3 atm ($N_2 : H_2 = 1 : 3$, 40 ml min^{-1}) for Ru/SiO_2. The normalized transient obtained for Cs–Ru/MgO under identical conditions is also included for comparison. For clarity, not all points are shown.

DISCUSSION

The number of active sites for metal catalysis is usually assumed equal to the total number of metal surface atoms counted by titration methods such as CO or H_2 chemisorption. However, it is very likely that chemisorption overestimates the actual number of active sites. A structure-sensitive reaction such as ammonia synthesis is particularly susceptible to an overcounting of active sites since specific ensembles of surface atoms are required to dissociate dinitrogen. Steady-state isotopic transient kinetic analysis is useful for probing the sites active for ammonia synthesis since the method involves the interrogation of an operating catalyst.

Nwalor and Goodwin measured a turnover frequency based on H_2 chemisorption (TOF_H) of 6×10^{-5} s^{-1} at 673 K and total pressure of 2 atm ($P_{NH_3} = 0.00064$ atm) for a 2.7 wt% Ru/SiO_2 catalyst and dispersion of 0.27 (8). Although their Ru loading was an order of magnitude lower than our Ru/SiO_2 sample, the results reported in the current work (7×10^{-5} s^{-1} at 673 K and total pressure of 3 atm) are in excellent agreement. However, the intrinsic turnover frequency (TOF_{intr}) at 673 K determined from SSITKA was about a factor of 3 higher for our 22 wt% Ru/SiO_2 catalyst compared to their catalyst (17×10^{-4} s^{-1} compared to 5.6×10^{-4} s^{-1}). The corresponding fractional coverage of nitrogen-containing intermediates was therefore a factor of 3 lower for our sample (0.023 compared to 0.067) based on total H_2 chemisorption. Nevertheless, Nwalor and Goodwin and the current work show conclusively that the intrinsic activity of Ru/SiO_2 is extremely low compared to promoted Ru catalysts.

The analysis performed in this work assumes that the rate of ammonia synthesis can be described by the expression

$$\text{rate} = k\theta_{NH_x}, \qquad [4]$$

where k is a pseudo-first-order rate constant and x ranges from 0 to 3. Additional discussion regarding the assumption of pseudo-first-order rates in SSITKA is provided by Shannon and Goodwin (19). Since the fractional surface coverage of NH_x species was similar on the Cs–Ru/MgO and Ru/SiO_2 catalyst examined in the present study, the difference in activity between the two catalysts must be due to a change in the intrinsic rate constant k. This is clearly evident by the two orders of magnitude increase of the TOF_{intr} for the Cs–Ru/MgO catalyst compared to Ru/SiO_2 at 40 ml min^{-1} and 673 K, even through the partial pressure of ammonia is a factor of 20 higher for the Cs–Ru/MgO catalyst. Apparently the enhancement of the rate over Cs-promoted Ru/MgO is electronic in nature, since the number of active sites is similar to Ru/SiO_2.

The fractional surface coverage of nitrogen-containing intermediates on our Cs-promoted Ru/MgO sample was much lower than that obtained on a commercial iron-based catalyst (Haldor Topsoe KMIR) under similar reaction conditions (17). Nwalor *et al.* found a fractional surface coverage of 0.73 (based on BET surface area measurements) at 673 K and a total pressure of 2 atm ($P_{NH_3} = 0.0042$). This is not surprising since the kinetics of ammonia synthesis over and iron and ruthenium are very different, with the iron surface being predominantly covered with nitrogen under ammonia synthesis conditions. We also found that the coverage on our Cs–Ru/MgO sample was much less than that reported for a K-promoted Ru/SiO_2 catalyst analyzed by the same technique (18). For K–Ru/SiO_2 at 673 K and 2 atm total pressure, the fractional surface coverage of NH_x was found to be 0.34, which is almost an order of magnitude greater than the coverage on Cs–Ru/MgO. Also, the intrinsic turnover frequency (TOF_{intr}) at 673 K determined from SSITKA was a factor of 16 higher for our Cs-promoted Ru/MgO catalyst compared to K-promoted Ru/SiO_2 (0.14 s^{-1} compared to 0.0088 s^{-1}). The lower activity of K–Ru/SiO_2 is presumably due to the reaction of the potassium promoter with the silica support and the lower basicity of potassium compounds relative to cesium compounds.

Finally, the impact of reaction reversibility ($2NH_3 \rightarrow N_2 + 3H_2$) on the SSITKA parameters needs to be addressed. Due to the lack of evidence for dinitrogen scrambling and since readsorption of ammonia was negligible, dinitrogen that participated in multiple reactions ($N_2 \rightarrow NH_3 \rightarrow N_2$) could be ignored. However, the effect of reaction reversibility should become more problematic at equilibrium conversion and low space velocities, where readsorption might be significant.

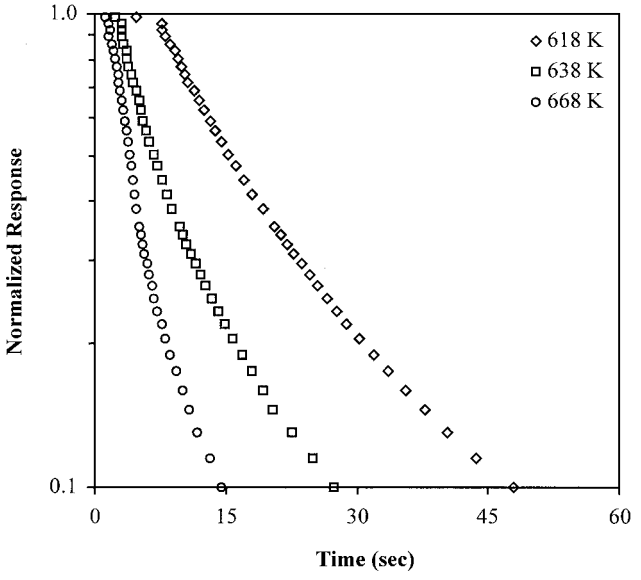

FIG. 10. Normalized transients of $^{15}NH_3$ at various temperatures at constant ammonia ($P_{NH_3} = 0.011$ atm) for Cs–Ru/MgO.

Although methods such as linear modeling have been developed for determination of kinetic parameters from SSITKA experiments (27), these techniques become rather complicated in cases where reaction reversibility is present. An additional complication is added due to the presence of ammonia readsorption on the system. However, a simple method for evaluating active site distributions is to plot the logarithm of the normalized transient as a function of time. Figure 10 illustrates the results from Runs 4–6 on Cs–Ru/MgO at three different temperatures but with constant ammonia pressure. Each transient in Fig. 10 is well represented by a single exponential decay, which suggests a uniform site distribution for the Cs–Ru/MgO catalyst. A similar result was found for the Ru/SiO_2 catalyst, as seen in Fig. 11. The data for Cs–Ru/MgO at the same conditions are included in Fig. 11 for comparison. Nwalor and Goodwin reported that the addition of K to Ru/SiO_2 created a class of superactive sites on the catalyst (18). Even though the new superactive sites constituted only 20% of the total number of sites on the promoted catalyst, they accounted for 78% of the observed reaction rate.

For iron-based ammonia synthesis catalysts, it is generally accepted that C_7 sites (Fe atoms with seven nearest neighbors) that are prevalent on the Fe(111) surface are responsible for the high catalytic activity. The possible structure sensitivity of ammonia synthesis on supported Ru particles is therefore of paramount importance. Dinitrogen activation on a Ru single crystal was recently found to be totally dominated by the steps on the surface, which act as low-barrier channels to populate terraces (28, 29). This so-called B_5 site is believed to be responsible for the high activity of ruthenium catalysts. The B_5 site consists of three ruthenium atoms in one layer and two atoms directly above this layer at a monoatomic step on a Ru(0001) terrace. Dissociation of NO was also found to occur exclusively at the steps of Ru(0001), with the population of the terraces occurring via diffusion (30).

The results from these single-crystal studies were then used as the basis for a microkinetic model of ammonia synthesis of a working catalyst. Dahl *et al.* found that 8–9% of the surface ruthenium atoms measured by dihydrogen chemisorption could correctly account for ammonia synthesis over $Ru/MgAl_2O_4$ and Ru/MgO catalysts (31). They were able to reproduce experimentally obtained results over the $Ru/MgAl_2O_4$ catalyst for ammonia pressures ranging over 3 orders of magnitude. They concluded that the surface was predominantly covered with NH^*, with the ratio between $\theta_N : \theta_{NH_3} : \theta_{NH_2} : \theta_{NH}$ being approximately 1 : 1 : 10 : 50. Their results suggest that NH^* is the energetically favored form of nitrogen-containing intermediates on the surface, which was recently confirmed by DFT calculations (32) and is consistent with reports in the surface science literature (33–35). At low ammonia partial pressures, adsorbed hydrogen competes for active sites whereas the coverage of nitrogen-containing species increases at higher ammonia levels.

Jacobsen *et al.* (36) recently counted the relative number of B_5 sites on ruthenium clusters using crystal models which expose only (001) and (100) hcp surface planes; the trend was similar to that presented earlier by van Hardeveld and van Montfoort for nickel crystallites (37). These models can be used to predict the optimal size of ruthenium particles needed to obtain the maximum number of B_5-type surface sites. The fraction of active surface ruthenium atoms

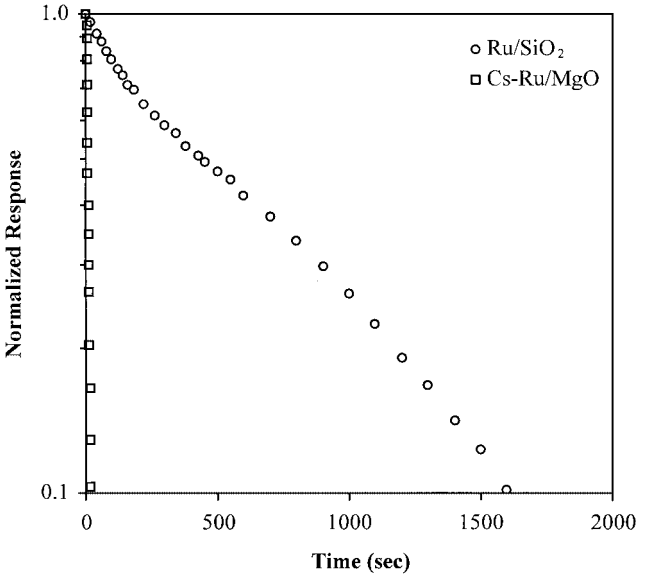

FIG. 11. Normalized transient of $^{15}NH_3$ at 673 K and 3 atm ($N_2 : H_2 = 1 : 3$, 40 ml min^{-1}) for Ru/SiO_2 and Cs-promoted Ru/MgO.

determined from our SSITKA measurements was about a factor of two to three lower than that predicted by the single-crystal models (36). This might be due to the crystal morphology assumed by Jacobsen *et al.* in determining the number of B_5 sites or to the crystal size distribution of our catalysts. To address the first issue, it should be noted that Jacobsen *et al.* assumed ideal surface models, which may overpredict the number of so-called B_5 sites of a working catalyst. Datye *et al.* have shown, using transmission electron microscopy, that the shape of Ru clusters on magnesia and silica depends on their size, with smaller crystallites being spherical and larger crystallites being ellipsoidal in shape (38). In addition, clusters smaller than 1 nm in diameter expose very few B_5 sites. Therefore, if a substantial fraction of our ruthenium particles is less than this critical size, they may be relatively inactive for N_2 dissociation although they are titrated by H_2 chemisorption.

Another possible source of discrepancy might be the determination of our ruthenium particle size. In some cases, hydrogen chemisorption on Ru can be unreliable in determining dispersion and therefore particle size (36, 39). However, our results from EXAFS analysis and dihydrogen chemisorption give approximately the same average particle size for the two catalysts in this study.

Ruthenium catalysts for ammonia synthesis are known to be inhibited by dihydrogen, especially at low ammonia pressure (18, 24, 25). Thus the competition for active surface sites by H_2 may lower the fractional coverage of nitrogen-containing intermediates determined in this work below that of the total active site concentration.

The role of basic supports and/or promoters such as alkali metal and alkaline earth compounds has been debated in the literature. Some believe that basic compounds lower the activation barrier for N_2 dissociation while others believe they reduce the coverage of nitrogen-containing intermediates, thus freeing sites for dinitrogen dissociation. Recent DFT calculations have shown that a promoter can only exert a significant influence on the activity if it is situated in the immediate vicinity of the sites for dissociation (40, 41). The presence of alkali metal on the Ru(0001) surface apparently lowers the barrier for N_2 dissociation through a direct electrostatic interaction. This is consistent with the higher rate of dinitrogen isotopic exchange found over Cs-promoted Ru/MgO compared to an unpromoted catalyst (6). However, it has also been shown that various alkali metals adsorbed on Ru(0001) destabilize NH_3^* and, presumably, have the same effect on NH^* and NH_2^* as well (31, 42, 43). Szmigiel *et al.* found the onset of ammonia formation during temperature-programmed surface reaction to be lower on Cs-promoted Ru/MgO compared to an unpromoted sample. In addition, they found the reaction order in ammonia changed from −0.5 to nearly zero when Ru/MgO was promoted with Cs (26). Similar results were found for Cs-promoted Ru/carbon catalysts (44).

Dahl *et al.* summarized nicely the periodic trends found in transition metal catalyzed ammonia synthesis (45). Results from density functional theory suggest that promoters decrease the barrier for N_2 dissociation *and* destabilize surface-bound nitrogen-containing intermediates. The relative importance of each effect depends on the type of metal used. Dahl *et al.* suggest that the promotional effect on Ru metal results mainly from a lower barrier for N_2 dissociation since the surface coverage of nitrogen-containing intermediates is very low. Indeed, the reaction kinetics of ammonia synthesis (nearly-1 order in H_2 and weakly inhibited by NH_3) over supported Ru are consistent with this idea.

From our results, it appears that the Cs–MgO combination increases the intrinsic turnover frequency of the active Ru sites compared to SiO_2 by an electronic effect that lowers the barrier for N_2 dissociation since the surface coverage of nitrogen-containing intermediates was about the same for both the highly active Cs–Ru/MgO and a poorly active Ru/SiO_2 catalyst. As mentioned earlier, the observed zero-order dependence of the rate on ammonia pressure suggests that the nitrogen-containing intermediates are not competing for active sites on Cs–Ru/MgO. Although the silica-based catalyst may be somewhat inhibited by product at higher ammonia partial pressures, it is not likely that product inhibition can totally account for the two orders of magnitude lower turnover frequency. Since dinitrogen dissociation is generally accepted as the rate-determining step, basic promoters appear to facilitate activation of dinitrogen over Ru.

CONCLUSIONS

Steady-state isotopic transient kinetic analysis (SSITKA) was used to determine the role of basic promoter/support for ammonia synthesis on a Cs-doped 1.75 wt% Ru/MgO catalyst. SSITKA was used to evaluate the intrinsic turnover frequency (TOF_{intr}) and surface concentration of nitrogen-containing intermediates (N_{NH_x}) leading to ammonia. The fractional surface coverage of nitrogen-containing intermediates (θ_{NH_x}) based on total H_2 chemisorption never exceeded 6% under the conditions examined. Similar surface coverages were found on a 22 wt% Ru/SiO_2 catalyst, which suggests that the role of basic supports and/or promoters is electronic in nature. This was evident by the two orders of magnitude increase in the TOF_{intr} over the Cs-promoted Ru/MgO catalyst as compared to unpromoted Ru/SiO_2. These results can be rationalized by a lower barrier for N_2 dissociation on base-promoted Ru.

ACKNOWLEDGMENTS

This work was supported by a grant from the National Science Foundation (CTS-9729812). Helpful discussions with Prof. James Goodwin regarding the transient experiments are also acknowledged. Research was

carried out in part at the National Synchrotron Light Source, Brookhaven National Laboratory, which is supported by the U.S. Department of Energy, Division of Materials Sciences and Division of Chemical Sciences (DOE Contract DE-AC02-76CH00016).

REFERENCES

1. Bielawa, H., Hinrichsen, O., Birkner, A., and Muhler, M., *Angew. Chem. Int. Ed.* **40**, 1061 (2001).
2. Chementator, *Chem. Eng.* **3**, 19 (1993).
3. Jacobsen, C. J. H., *Chem. Commun.* 1057 (2000).
4. Aika, K., Ohya, A., Ozaki, A., Inoue, Y., and Yasumori, I., *J. Catal.* **92**, 305 (1985).
5. Aika, K.-I., Takano, T., and Murata, S., *J. Catal.* **136**, 126 (1992).
6. Hinrichsen, O., Rosowski, F., Hornung, A., Muhler, M., and Ertl, G., *J. Catal.* **165**, 33 (1997).
7. Happel, J., *Chem. Eng. Sci.* **33**, 1567 (1978).
8. Rothaemel, M., Hanssen, K. F., Blekkan, E. A., Schanke, D., and Holmen, A., *Catal. Today* **38**, 79 (1997).
9. Agnelli, M., Swaan, H. M., Marquez-Alvarez, C., Martin, G. A., and Mirodatos, C., *J. Catal.* **175**, 117 (1998).
10. Ali, S. H., and Goodwin, J. G., Jr., *J. Catal.* **176**, 3 (1998).
11. Bajusz, I.-G., and Goodwin, J. G., Jr., *J. Catal.* **169**, 157 (1997).
12. De Pontes, M., Yokomizo, G. H., and Bell, A. T., *J. Catal.* **104**, 147 (1987).
13. Haddad, G. J., Chen, B., and Goodwin, J. G., Jr., *J. Catal.* **161**, 274 (1996).
14. Efstathiou, A. M., and Verykios, X. E., *Appl. Catal. A* **151**, 109 (1997).
15. Ali, S. H., and Goodwin, J. G., Jr., *J. Catal.* **170**, 265 (1997).
16. Ali, S. H., and Goodwin, J. G., Jr., *J. Catal.* **171**, 339 (1997).
17. Nwalor, J. U., Goodwin, J. G., Jr., and Biloen, P., *J. Catal.* **117**, 121 (1989).
18. Nwalor, J. U., and Goodwin, J. G., Jr., *Top. Catal.* **1**, 285 (1994).
19. Shannon, S. L., and Goodwin, J. G., Jr., *Chem. Rev.* **95**, 677 (1995).
20. McClaine, B. C., Siporin, S. E., and Davis, R. J., *J. Phys. Chem. B* **105**, 7525 (2001).
21. Greegor, R. B., and Lytle, F. W., *J. Catal.* **63**, 476 (1980).
22. Clausen, B. S., Grabaek, L., Topsoe, H., Hansen, L. B., Stoltze, P., Norskov, J. K., and Nielsen, O. H., *J. Catal.* **141**, 368 (1993).
23. Gao, S., and Schmidt, L. D., *J. Catal.* **115**, 356 (1989).
24. Becue, T., Davis, R. J., and Garces, J. M., *J. Catal.* **179**, 129 (1998).
25. McClaine, B. C., Becue, T., Lock, C., and Davis, R. J., *J. Mol. Catal. A* **163**, 105 (2000).
26. Szmigiel, D., Bielawa, H., Kurtz, M., Hinrichsen, O., Muhler, M., Rarog, W., Jodzis, S., Kowalczyk, Z., Znak, L., and Zielinski, J., *J. Catal.* **205**, 205 (2002).
27. Shannon, S. L., and Goodwin, J. G., *Appl. Catal. A* **151**, 3 (1997).
28. Dahl, S., Logadottir, A., Egeberg, R. C., Larsen, J. H., Chorkendorff, I., Tornqvist, E., and Norskov, J. K., *Phys. Rev. Lett.* **83**, 1814 (1999).
29. Dahl, S., Tornqvist, E., and Chorkendorff, I., *J. Catal.* **192**, 381 (2000).
30. Zambelli, J., Trost, J., Wintterlin, J., and Ertl, G., *Phys. Rev. Lett.* **76**, 795 (1996).
31. Dahl, S., Sehested, J., Jacobsen, C. J. H., Tornqvist, E., and Chorkendorff, I., *J. Catal.* **192**, 391 (2000).
32. Rod, T. H., Logadottir, A., and Norskov, J. K., *J. Chem. Phys.* **112**, 5343 (2000).
33. Dietrich, H., Jacobi, K., and Ertl, G., *J. Chem. Phys.* **106**, 9313 (1997).
34. Dietrich, H., Jacobi, K., and Ertl, G., *Surf. Sci.* **352–354**, 138 (1996).
35. Shi, H., Jacobi, K., and Ertl, G., *J. Chem. Phys.* **102**, 1432 (1995).
36. Jacobsen, C. J. H., Dahl, S., Hansen, P. L., Tornqvist, E., Jensen, L., Topsoe, H., Prip, D. V., Moenshaug, P. B., and Chorkendorff, I., *J. Mol. Catal. A* **163**, 19 (2000).
37. van Hardeveld, R., and van Montfoort, A., *Surf. Sci.* **4**, 396 (1966).
38. Datye, A. K., Logan, A. D., and Long, N. J., *J. Catal.* **109**, 76 (1988).
39. Kowalczyk, Z., Jodzis, S., Rarog, W., Zielinski, J., and Pielaszek, J., *Appl. Catal. A* **173**, 153 (1998).
40. Mortensen, J. J., Hammer, B., and Norskov, J. K., *Phys. Rev. Lett.* **80**, 4333 (1998).
41. Mortensen, J. J., Hammer, B., and Norskov, J. K., *Surf. Sci.* **414**, 315 (1998).
42. Dietrich, H., Jacobi, K., and Ertl, G., *Surf. Sci.* **377–379**, 308 (1997).
43. Benndorf, C., and Madey, T. E., *Chem. Phys. Lett.* **101**, 59 (1983).
44. Rarog, W., Kowalczyk, Z., Sentek, J., Skladanowski, D., Szmigiel, D., and Zielinski, J., *Catal. Lett.* **68**, 163 (2000).
45. Dahl, S., Logadottir, A., Jacobsen, C. J. H., and Norskov, J. K., *Appl. Catal. A* **222**, 19 (2001).